

# Cooperative Interference-Aware Joint Scheduling for the 3GPP LTE Uplink

Philipp Frank\*, Andreas Müller<sup>‡</sup>, Heinz Droste\* and Joachim Speidel<sup>‡</sup>

\*Deutsche Telekom Laboratories, Berlin, Germany

<sup>‡</sup>Institute of Telecommunications, University of Stuttgart, Germany

E-Mail: philipp.frank@telekom.de

**Abstract**—In current cellular networks base stations (BSs) usually perform independent scheduling without coordinating the resource allocation among different cells. This, however, often leads to high interference levels in cellular networks operating with universal frequency reuse, such as the 3GPP UTRAN Long Term Evolution (LTE). Coordinated scheduling between different BSs may mitigate this problem by taking interference from and to nearby BSs into account in order to avoid high interference situations, especially for user equipments (UEs) located near the cell-edge. For that purpose, we propose in this paper a novel interference-aware joint scheduling scheme based on proportional fairness for the uplink of a 3GPP UTRAN LTE system, where different BSs cooperate with each other via a fast backhaul network in order to jointly allocate frequency resources to the various UEs, taking the caused inter-cell interference into account. Furthermore, we propose an efficient method for dynamic interference coordination based on the standardized high interference indicator and we compare the achievable performance with this approach to a system with interference-aware joint scheduling. It is shown that our joint scheduling scheme outperforms a dynamic interference coordination scheme and that it yields significant gains over a conventional LTE Release 8 system without any interference coordination.

## I. INTRODUCTION

Recently, interference coordination has emerged as one of the most attractive techniques for combating interference in next generation cellular networks (see for example [1]–[5]), such as the 3GPP UTRAN Long Term Evolution (LTE), which operates with universal frequency reuse in order to exploit the whole frequency bandwidth in each cell. The main drawback of universal frequency reuse systems is, however, inter-cell interference caused by simultaneous transmissions scheduled on the same frequency resources by nearby base stations (BSs), particularly limiting the performance of user equipments (UEs) located at the cell-edge, which suffer most from inter-cell interference. In order to partially mitigate this problem, a cooperation among adjacent BSs may be employed for coordinating the inter-cell interference by jointly allocating radio resources to the various UEs located within the respective cooperation cluster.

On the one hand, such an interference coordination may be realized in a static manner by means of fractional frequency reuse, for example, where different parts of the available bandwidth are only accessible to certain UEs depending on whether they are located at the cell-center or the cell-edge [1], [3]. To this end, fixed restrictions on the assignable frequency resources are introduced, so that the cell-edge UEs of adjacent

BSs are not allocated to the same part of the frequency bandwidth, thus avoiding severe inter-cell interference. However, a general problem of fixed allocation restrictions is the reduced availability of assignable frequency resources and the inherent reduction of the frequency diversity.

On the other hand, dynamic schemes for coordinating inter-cell interference only impose restrictions on certain frequency resources when high interference is expected, what consequently leads to a more efficient utilization of the available frequency spectrum [1], [4], [5]. For that purpose, adjacent BSs inform each other about upcoming resource allocations of cell-edge UEs, so that this information can be taken into account in the scheduling decisions in order to limit the impact of the inter-cell interference on the system performance. However, even with such a dynamic scheme the achievable performance is generally still worse than with global joint scheduling across a set of cooperating BSs, where channel state information (CSI) of all associated UEs is considered.

For this reason we propose in this paper a novel frequency-selective proportional fair joint scheduling algorithm, where the resource allocation is performed in a cooperative fashion by a central scheduling unit for a set of cooperating BSs. Please note that this central scheduling unit may be incorporated in one of the cooperating BSs, which we assume to be connected with any of the other cooperating BSs via a fast high-capacity backhaul network. This way, multi-cell CSI of all UEs associated with the set of cooperating BSs can be periodically exchanged in order to predict the experienced inter-cell interference level if a certain UE would be scheduled on certain physical resource blocks (PRBs). This information is then considered in the scheduling decisions for minimizing the inter-cell interference, leading to an interference-aware scheduling. In order to compare the system performance of our joint scheduling scheme to a state-of-the-art LTE interference coordination scheme, we propose an efficient method for dynamically coordinating the inter-cell interference based on the standardized high interference indicator (HII) signaling between cooperating BSs [1], [2], [6]. We analyze the system performance of both proposed schemes by means of extensive system-level simulations and we compare the achievable gains over a conventional system without interference coordination.

The remainder of this paper is organized as follows: In Section II, we highlight our reference proportional fair scheduling mechanism. Then, the proposed dynamic interference coordi-

nation as well as interference-aware joint scheduling schemes are outlined in more detail in Section III and IV, respectively. In Section V, we briefly describe our simulation methodology and selected system-level simulation results are shown, before finally our conclusions are given in Section VI.

## II. PROPORTIONAL FAIR SCHEDULING MECHANISM

In the following, we outline the basic principle of frequency-domain channel-aware proportional fair scheduling, considering the uplink of a 3GPP LTE Release 8 system with single-carrier frequency division multiple access (SC-FDMA). In order to exploit the multi-user diversity as well as the frequency selectivity of the channel, CSI of the associated UEs over the whole frequency bandwidth is required at the BS side. To this end, demodulation reference signals are transmitted along with the actual data as well as along with the control signals in order to facilitate coherent detection at the BS side. Furthermore, the BSs schedule sounding reference signals to obtain CSI of those frequency bandwidth parts, which are not associated with any uplink data transmission, thus enabling channel dependent scheduling.

Having estimates of the uplink channel, the BSs can determine the proportional fair metric for each of the associated UEs and each PRB, where one PRB is considered to be the minimum resource unit for subcarrier allocation. Proportional fairness among the UEs is guaranteed through realizing a reasonable trade-off between maximal total throughput and cell-edge throughput, thus selecting UEs with the instantaneous highest supportable throughput relative to its long-term average throughput given by [7]

$$G_{i,j}(k) = \frac{R_{i,j}(k)}{T_i^\alpha(k)}, \quad (1)$$

with  $G_{i,j}(k)$  as the scheduling priority for the  $i$ -th UE on the  $j$ -th PRB during the transmission time interval (TTI)  $k$ ,  $R_{i,j}(k)$  as the instantaneous supportable throughput and  $\alpha$  as the fairness factor, which determines the trade-off between efficiency in terms of total throughput and fair scheduling. Furthermore,  $T_i(k)$  denotes the long-term average throughput given by

$$T_i(k+1) = \begin{cases} \beta T_i(k) & i \notin \Omega(k) \\ \beta T_i(k) + (1-\beta) R_i(k) & i \in \Omega(k) \end{cases}, \quad (2)$$

where  $\beta$  denotes the forgetting factor and  $\Omega(k)$  as well as  $R_i(k)$  denote the set of scheduled UEs at TTI  $k$  and the aggregated throughput of the scheduled UE  $i$ , respectively. Based on the scheduling priorities in (1), the PRB allocation is performed according to the algorithm presented in [8]. In contrast to the downlink, where orthogonal frequency division multiplexing (OFDM) is used as access scheme, the resource allocation in the uplink is generally more complex since SC-FDMA only allows allocated subcarriers (PRBs) to be either adjacent or evenly spaced in order to achieve a low peak-to-average power ratio [9], leading to a significantly reduced allocation flexibility. For this reason, the fundamental idea in [8] is to start the resource allocation with the PRB associated

with the highest scheduling priority and assign adjacent PRBs until either a different UE has a higher scheduling priority or the maximum transmit power is reached. This way, the UEs are approximately assigned according to the envelope of the scheduling priorities, thus exploiting the multi-user diversity as well as the frequency selectivity of the channel while taking the allocation constraints due to SC-FDMA into account.

## III. DYNAMIC INTERFERENCE COORDINATION

In order to facilitate a dynamic interference coordination between different BSs, we make use of the standardized proactive LTE HII. This HII consists of a bitmap with one bit per PRB and provides information about upcoming uplink transmissions of cell-edge UEs, which thus may cause high interference to adjacent BSs [6]. Hence, this information can be taken into account for improving the system performance, particularly at the cell-edge. For realizing a fast adaptation to the current interference situation, each BS periodically sends a dedicated HII report to its corresponding set of cooperating BSs via a high-capacity backhaul network, which may be realized by means of the X2 interface.

In this regard, we first of all assume that each BS identifies its cell-edge UEs based on their reported reference signal received power (RSRP) measurements [10], which are mainly used for handover decisions in conventional LTE systems. Hence, the  $i$ -th UE is selected as a cell-edge UE if the following condition is met

$$\zeta_{i,m} [\text{dBm}] < \rho [\text{dBm}], \quad m \in C_l, \quad (3)$$

where  $\zeta_{i,m}$  denotes the reported long-term attenuation of the channel between the  $i$ -th UE assigned to its serving BS  $l$  and the  $m$ -th BS,  $\rho$  denotes a predefined threshold value and the set of cooperating BSs associated with the BS  $l$  is indicated by  $C_l$ .

Each BS reserves certain PRBs on which its cell-edge UEs have to be allocated during a certain reporting time interval until a new HII report is signaled to the corresponding set of cooperating BSs. This way, severe inter-cell interference caused by UEs located near the cell border of other BSs becomes predictable. In order to allow for a flexible frequency-selective scheduling, the resource allocation restrictions of the cell-edge UEs are updated after each reporting time interval, taking their current channel conditions into account.

Having received the HII reports of the cooperating BSs, the impact of the inter-cell interference can be limited either by scheduling only cell-center UEs on the reported PRBs, which are less affected by high interference levels, or by not scheduling any UE on these PRBs. Since in the latter case the resource allocation flexibility is reduced, we select for each reported high interference PRB a set of UEs, which can be assigned to these PRBs without being significantly affected by the expected high interference level. Let us assume in the following that all BSs are equipped with  $N$  antenna elements, whereas all UEs have only a single antenna element. Then, the UEs allowed to be scheduled on the reported high interference

PRBs are selected according to

$$\frac{1}{Q} \sum_{q=1}^Q \left\| \sqrt{P_i} \mathbf{h}_{q,i} \right\| > \eta, \quad i \in M_l, \quad (4)$$

with  $Q$  as the number of subcarriers per PRB,  $P_i$  as the transmit power per subcarrier of the  $i$ -th UE,  $\mathbf{h}_{q,i}$  as the  $N$ -dimensional channel vector from the  $i$ -th UE to its serving BS  $l$ ,  $M_l$  as the set of UEs assigned to BS  $l$ ,  $\eta$  as a predefined channel quality threshold and  $\|\cdot\|$  as the Euclidean norm. Depending on the actual value of the channel quality threshold  $\eta$ , the inter-cell interference can be coordinated in such a way that cell-edge UEs associated to different BSs are not scheduled on the same PRBs, thus in particular improving the interference situation for these UEs.

#### IV. INTERFERENCE-AWARE JOINT SCHEDULING

We extend the proportional fair mechanism outlined in Section II in such a way that different BSs may jointly perform resource allocation in order to improve the system performance. A crucial prerequisite for the proposed joint scheduling scheme is that multi-cell CSI is periodically signaled from the cooperating BSs to a central scheduling unit, which may be incorporated in one of the cooperating BSs in order to enable a smooth integration into the here considered 3GPP LTE Release 8 architecture. For that purpose, we assume that each scheduling unit is interconnected with its corresponding cooperating BSs via high-capacity low-latency backhaul links.

Each central scheduling unit performs the resource allocation according to Fig. 1, which depicts the flow chart of our proposed joint scheduling algorithm. After processing the requested retransmissions by a hybrid automatic repeat request (HARQ) protocol, the cooperating BSs are ordered by means of a certain fairness criterion, which will be outlined in more detail at the end of this section. Then, the frequency resources are allocated to the various UEs based on the exchanged multi-cell CSI, considering not only the current channel conditions between these UEs and their serving BSs, but also the expected inter-cell interference caused by assigning these UEs to certain PRBs. As illustrated in Fig. 1, resource allocation is carried out stepwise for each set of UEs assigned to one of the cooperating BSs in order to reduce the computational complexity. Hence, the joint scheduling priority for the  $j$ -th PRB and  $i$ -th UE associated to its serving BS  $l$  can be determined as follows

$$S_{i,j}(k) = G_{\Psi_j,i,j}(k) + \sum_{n \in \Psi_j} G_{\Lambda_j,n,j}(k), \quad i \in M_l, \quad (5)$$

with  $M_l$  as the set of UEs assigned to BS  $l$ ,  $\Psi_j$  as the set of already scheduled UEs on the PRB  $j$  and  $G_{\Psi_j,i,j}(k)$  as the scheduling priority for the  $i$ -th UE allocated to the  $j$ -th PRB on which already the set of UEs  $\Psi_j$  are scheduled. Furthermore,  $G_{\Lambda_j,n,j}(k)$  denotes the scheduling priority for the  $n$ -th UE and  $j$ -th PRB, taking into account that the  $i$ -th UE will be scheduled on the  $j$ -th PRB, where the set of UEs  $\Lambda_j = \{\Psi_j \setminus \{n\}, i\}$  are causing inter-cell interference. In the following, we explicitly outline the calculation of the

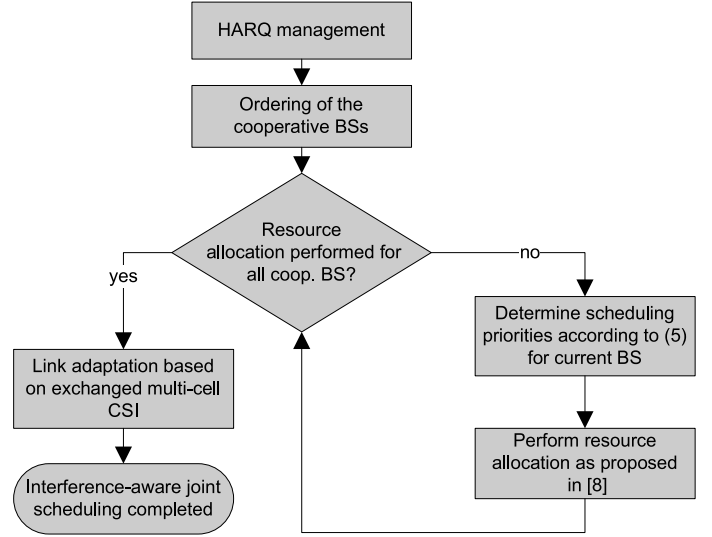


Fig. 1. Flow chart of the interference-aware joint scheduling algorithm.

scheduling priority  $G_{\Lambda_j,n,j}(k)$  only, but it should be noted that the scheduling priority  $G_{\Psi_j,i,j}(k)$  can be determined in a rather straightforward manner. According to (1), the scheduling priority  $G_{\Lambda_j,n,j}(k)$  is given by

$$G_{\Lambda_j,n,j}(k) = \frac{R_{\Lambda_j,n,j}(k)}{T_n^\alpha(k)}, \quad (6)$$

where the instantaneous supportable throughput  $R_{\Lambda_j,n,j}(k)$  is estimated by means of the Shannon capacity formula as follows

$$R_{\Lambda_j,n,j}(k) = \frac{1}{Q} \sum_{q=1}^Q \log_2(1 + \gamma_{n,j,q}). \quad (7)$$

The number of subcarriers per PRB as well as the SINR are denoted by  $Q$  and  $\gamma_{n,j,q}$ , respectively. As already mentioned before, we assume that we have single-antenna UEs and that all BSs are equipped with  $N$  antenna elements. Then, the SINR  $\gamma_{n,j,q}$  for the  $n$ -th UE and the  $q$ -th subcarrier of the  $j$ -th PRB can be expressed as

$$\gamma_{n,j,q} = \frac{P_n \mathbf{w}_{n,j,q} \mathbf{h}_{n,j,q} \mathbf{h}_{n,j,q}^\dagger \mathbf{w}_{n,j,q}^\dagger}{\mathbf{w}_{n,j,q} \mathbf{R}_{zz} \mathbf{w}_{n,j,q}^\dagger}, \quad (8)$$

with  $P_n$  as the transmit power per subcarrier of UE  $n$ ,  $\mathbf{h}_{n,j,q}$  as the  $N$ -dimensional channel vector from the  $n$ -th UE to its serving BS,  $\mathbf{w}_{n,j,q}$  as the corresponding weight vector for coherent detection and  $(\cdot)^\dagger$  as the conjugate-transpose operator. The covariance matrix of the interference plus noise is expressed by  $\mathbf{R}_{zz} = \mathbb{E}[\mathbf{i}_{n,j,q} \mathbf{i}_{n,j,q}^\dagger] + \mathbb{E}[\mathbf{n}_{n,j,q} \mathbf{n}_{n,j,q}^\dagger]$ , where  $\mathbf{i}_{n,j,q}$  denotes the inter-cell interference caused by the set of UEs  $\Lambda_j$  and  $\mathbf{n}_{n,j,q}$  the thermal noise. We consider a linear minimum mean square error (LMMSE) receiver for equalizing the received signal, thus the weight vector  $\mathbf{w}_{n,j,q}$  is given by

$$\mathbf{w}_{n,j,q} = \mathbf{h}_{n,j,q}^\dagger \left( \mathbf{h}_{n,j,q} \mathbf{h}_{n,j,q}^\dagger + \text{diag}(\mathbf{R}_{zz}) \right)^{-1}, \quad (9)$$

where  $\text{diag}(\cdot)$  denotes the diagonalization operator, which sets all elements of a matrix except for its main diagonal equal to zero. Based on the available multi-cell CSI, the central scheduling unit is able to predict the interference covariance matrix in (8) given by

$$\mathbf{R}_{ii} = \mathbb{E} \left[ \mathbf{i}_{n,j,q} \mathbf{i}_{n,j,q}^\dagger \right] = \sum_{m \in \Lambda_j} P_m \mathbf{h}_{m,j,q} \mathbf{h}_{m,j,q}^\dagger, \quad (10)$$

where  $\mathbf{h}_{m,j,q}$  denotes the  $N$ -dimensional channel vector from the  $m$ -th UE to the serving BS of UE  $n$ . Clearly,  $\mathbf{R}_{ii}$  in (10) contains both the inter-cell interference level caused by the already scheduled UEs associated to the cooperating BSs as well as the one that will be generated by assigning the  $i$ -th UE to the considered PRB. As a consequence, the joint scheduling priorities in (5) reflect the weighted sum throughput taking the current inter-cell interference situation into consideration.

Having determined the joint scheduling priorities of each PRB and UE, the resource allocation is then carried out according to [8] as illustrated in Fig. 1. Finally, after completing the resource allocation of all cooperating BSs, the link adaptation selects for each UE the spectrally most efficient modulation and coding scheme (MCS) that can be supported by its current uplink channel without exceeding a given target block error rate (BLER). For that purpose, the corresponding SINR is estimated by evaluating the available multi-cell CSI, resulting in a more accurate MCS selection compared to a conventional system without any cooperation.

As already mentioned before, each set of cooperating BSs is ordered in advance by the corresponding central scheduling unit in order to sustain fairness among the various UEs. To this end, the long-term BS throughput averaged across the number of assigned UEs is used as fairness criterion, which can be expressed for a certain BS  $l$  as

$$T_{\text{avg},l}(k+1) = \tau T_{\text{avg},l}(k) + (1-\tau) \frac{T_{\text{inst},l}(k)}{K_l}, \quad (11)$$

with  $T_{\text{avg},l}(k)$  as the long-term throughput for BS  $l$  at TTI  $k$ ,  $T_{\text{inst},l}(k)$  as the instantaneous throughput for BS  $l$ ,  $\tau$  as the forgetting factor and  $K_l$  as the number of UEs assigned to BS  $l$ . Consequently, the resource allocation always starts with the BS associated with the lowest long-term throughput and ends with the one associated with the highest long-term throughput.

## V. SIMULATION METHODOLOGY & RESULTS

The system performance of our proposed interference-aware joint scheduling scheme is thoroughly analyzed by means of extensive system-level simulations for a 3GPP LTE Release 8 cellular network, corresponding to a standard hexagonal grid consisting of seven BS sites with three sectors per site. The most important system parameters are given in Table I. Multi-path fading is modeled by means of the 3GPP spatial channel model (SCM) and we make use of the wrap around technique in order to avoid any border effects. Furthermore, we investigate the Urban Macro 1 and Macro 3 cases with inter-site distances of 500 m and 1732 m, respectively, and we apply the mutual information effective SINR mapping

TABLE I  
SYSTEM LEVEL SIMULATION PARAMETERS

Parameter	Setting
Deployment scenario	7 BS sites with 3 sectors per site
Inter-site distance (ISD)	500 m [Macro 1] or 1732 m [Macro 3]
Carrier freq. / bandwidth	2.0 GHz / 10 MHz
Channel model	3GPP SCM
Distance-dependent path loss	According to 3GPP TR 25.814 [13]
Shadowing standard deviation	8 dB
UE speed	3 kmph (quasi-static)
Avg. number of UEs/sector	10
Target BLER	10 %
UE / BS antennas	1 / 2 per sector
Traffic model	Infinite full buffer
HARQ	Synchronous, non-adaptive
Parallel HARQ processes	8 + X (X = additional delay in TTI)
Scheduling algorithm	Proportional-fair [8] (w/o cooperation) Interference-aware (w/ cooperation)
Scheduling fairness factor	$\alpha = 1$
Scheduling forgetting factor	$\beta = 0.97$
BS throughput forgetting factor	$\tau = 0.85$
Default joint scheduling delay	2 TTIs
CSI exchange interval	2 TTIs
HII reporting interval	10 TTIs
HII channel quality threshold	$\eta = 5 \cdot 10^{-8}$
Channel attenuation threshold	$\rho = -85$ dBm
Link-to-system interface	MIESM [11]
Power control	$P_0 = -58$ dBm, $\alpha = 0.6$ [Macro 1] $P_0 = -60$ dBm, $\alpha = 0.6$ [Macro 3] $P_{\text{max}} = 24$ dBm
BS receiver type	LMMSE
Channel estimation	Ideal
Control channel overhead	Upper and lower 4 PRBs
Reference signals overhead	According to 3GPP TS 36.211 [14]

(MIESM) for establishing the link-to-system interface [11]. The fast link adaptation can choose between several different modulation and coding schemes in order to dynamically adapt to the prevailing channel conditions of each UE and the given average target BLER is achieved by an additional outer loop link adaptation scheme presented in [12]. Besides, we consider an error-free but delayed data transmission across the backhaul links. The transmit power of a certain UE is set according to a simple open-loop power control scheme defined by

$$P_{\text{TX}} [\text{dBm}] = \min \{ P_{\text{max}}, P_0 + 10 \log_{10} M + \alpha \text{PL} \}, \quad (12)$$

with  $P_{\text{max}}$  as the maximum transmit power,  $P_0$  as a reference power,  $M$  as the number of assigned PRBs and  $\alpha$  as well as PL denote a constant path loss compensation factor and the long-term attenuation of the channel between the UE and its serving sector, respectively. Besides, retransmissions are processed by means of a synchronous, non-adaptive HARQ protocol with incremental redundancy. Due to the increased delay between scheduling and actual data transmission in case of the proposed joint scheduling scheme, we assume in the following that the HARQ timing and hence the number of parallel HARQ processes are adjusted so that the specified round-trip time for a HARQ protocol process is not exceeded.

Fig. 2 illustrates the system performance that can be achieved with the proposed interference-aware joint scheduling scheme, where all seven BS sites are interconnected with one single central scheduling unit, what is always assumed in

the following. As a result, the resource allocation is jointly performed across all BS sites of the considered deployment scenario. However, each BS sector in Fig. 2 has only multi-cell CSI of the UEs associated with its six surrounding cooperating sectors, thus only the inter-cell interference caused by these UEs can be taken into account for the resource allocation. If not stated otherwise, we also assume an additional delay of two TTIs introduced by signaling the scheduling decisions from the central scheduling unit to the corresponding BSs. Besides, both the average spectral efficiency and the cell-edge throughput defined as the 5<sup>th</sup> percentile of the UE throughput distribution are depicted in Fig. 2. It can be seen that the system performance and in particular the cell-edge throughput is significantly increased with the proposed interference-aware joint scheduling scheme. Since cell-edge UEs suffer most from inter-cell interference, they are the ones benefiting the most from the joint resource allocation. Moreover, Fig. 2 also shows the upper limits of the system performance if the exchange of the multi-cell CSI from the BSs to the central scheduling unit can be realized without any additional delay. Hence, the performance is not degraded due to a mismatch between the channels periodically determined during the multi-cell channel estimation stage at the BS sites and the ones used as the basis for the resource allocation at the central scheduling unit.

Fig. 3 illustrates the impact of the number of cooperating sectors on the system performance. As can be seen, the system performance steadily improves with increasing number of cooperating sectors for the Macro 1 as well as for the Macro 3 case. This is because not only the resource allocation of the various UEs becomes more accurate due the increased multi-cell CSI, but also the link adaptation. Since the link adaptation selects the appropriate MCSs based on the periodically exchanged multi-cell CSI, the prediction of the current interference levels can be considerably improved with increasing number of cooperating sectors, thus leading to a reduced probability of over- or underestimating the instantaneous MCS.

The system performance as a function of the overall bandwidth occupancy for the proposed joint scheduling as well as for the dynamic interference coordination scheme is shown in Fig. 4. In order to achieve a certain bandwidth occupancy, the scheduling is performed until the intended degree of bandwidth utilization is reached. First of all, it can be seen that our interference-aware joint scheduling scheme outperforms dynamic interference coordination due to the higher flexibility in jointly allocating PRBs to the various UEs, which consequently leads to an improved avoidance of severe inter-cell interference. The better system performance in case of interference-aware joint scheduling, however, comes at the cost of an increased backhaul load due to the required exchange of the multi-cell CSI<sup>1</sup>. Furthermore, we note that significant performance gains can be achieved with both the joint schedul-

<sup>1</sup>The required backhaul traffic demand in case of joint scheduling and interference coordination for the here considered scenario is about 200 Mbit/s and 25 kbit/s, respectively. A quantization granularity of 50 bit per resource allocation table and 16 bit per channel impulse response is assumed.

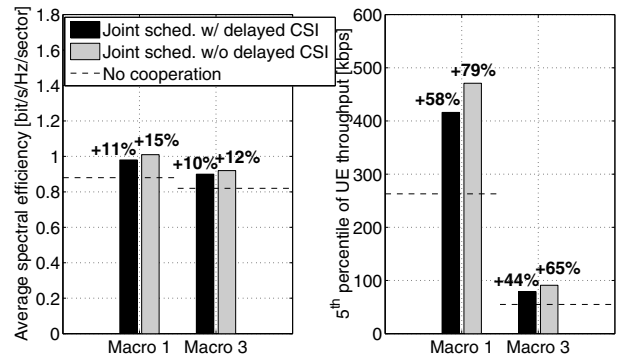


Fig. 2. System performance for the Macro 1 and Macro 3 case with interference-aware joint scheduling and six cooperating sectors. The given percentages denote the relative performance gains compared to a conventional system without cooperation.

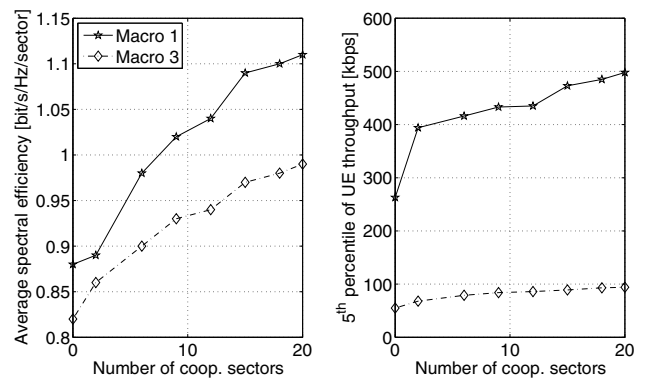


Fig. 3. Impact of the number cooperating sectors on the system performance for the Macro 1 and Macro 3 case.

ing as well as the dynamic interference coordination scheme compared to a system without cooperation. Interestingly, the gains increase with decreasing bandwidth occupancy what is also confirmed by Fig. 5, where the relative gains in terms of average spectral efficiency as well as cell-edge throughput are illustrated. This indicates that the flexibility in assigning PRBs to the various UEs is considerably increased at a low bandwidth occupancy. As a result, severe inter-cell interference situations can be avoided by exploiting the whole bandwidth, i.e. not allocating the same PRBs to the various UEs of the cooperating BSs.

Finally, Fig. 6 shows the impact of the additional delay introduced by our interference-aware joint scheduling scheme due to the exchange of the scheduling decisions between the central scheduling unit and the corresponding BSs. Clearly, with increasing delay the performance becomes steadily worse for all considered cases since the channels of the various UEs change during that time. Hence, the available multi-cell CSI at the central scheduling unit, which is used as input for the resource allocation as well as for the link adaptation, deviate more and more from the channels during the actual data transmission. For the cases with two and six cooperating

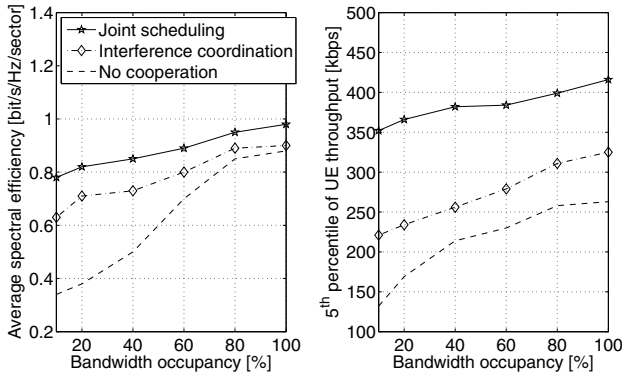


Fig. 4. System performance comparison between interference-aware joint scheduling and dynamic interference coordination dependent on the bandwidth occupancy for the Macro 1 case and six cooperating sectors.

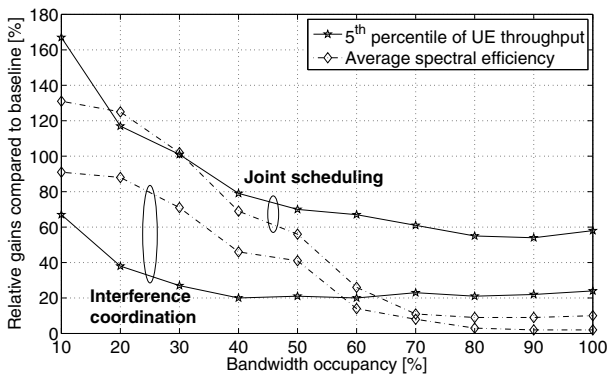


Fig. 5. Relative performance gains of interference-aware joint scheduling and dynamic interference coordination compared to a conventional system without cooperation for the Macro 1 case and six cooperating sectors.

sectors, the average spectral efficiency might even become worse than without any cooperation if the delay is too high. By contrast, significant gains in terms of cell-edge throughput can be achieved even with a delay of 10 TTIs for all considered cooperation cluster sizes.

## VI. CONCLUSION

We have presented a novel approach for jointly performing the resource allocation of various UEs associated to different cooperating BSs based on proportional fairness. By means of periodically exchanged multi-cell CSI between the cooperating BSs and a central scheduling unit via a fast high-capacity backhaul network it is possible to accurately predict the caused inter-cell interference level if a certain UE would be scheduled on certain PRBs, leading to an interference-aware scheduling. We have investigated the performance of our scheme by means of extensive system-level simulations for a 3GPP LTE system and it turned out that the system performance and in particular the cell-edge throughput can be significantly improved this way. Moreover, it is shown that our interference-aware joint scheduling scheme outperforms a state-of-the-art dynamic interference coordination scheme based on HII signaling and

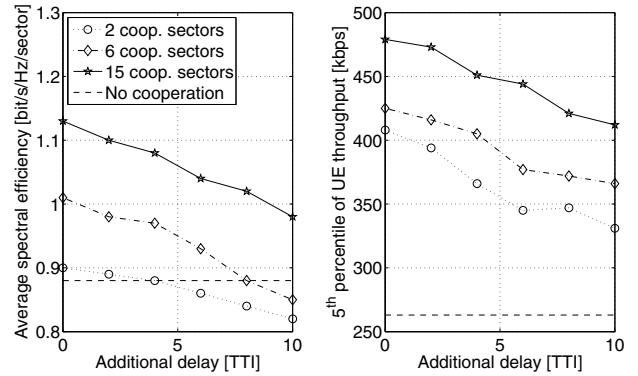


Fig. 6. Impact of the additional delay on the system performance due to scheduling information exchange for the Macro 1 case and three different cluster sizes.

therefore it represents a very attractive option for future LTE-Advanced systems.

## ACKNOWLEDGMENT

The authors acknowledge the excellent cooperation of all partners within the EASY-C project and the support by the German Federal Ministry of Education and Research (BMBF).

## REFERENCES

- [1] G. Boudreau, J. Panicker, N. Guo, R. Chang, N. Wang, and S. Vrzic, "Interference coordination and cancellation for 4G networks," *IEEE Commun. Mag.*, vol. 47, no. 4, pp. 74–81, Apr. 2009.
- [2] D. Astély, E. Dahlman, A. Furuskär, Y. Jading, M. Lindström, and S. Parkvall, "LTE: The evolution of mobile broadband," *IEEE Commun. Mag.*, vol. 47, no. 4, pp. 44–51, Apr. 2009.
- [3] F. Xiangning, C. Si, and Z. Xiaodong, "An inter-cell interference coordination technique based on users' ratio and multi-level frequency allocations," in *Proc. IEEE Wireless Commun., Networking and Mobile Computing Conf.*, Sep. 2007, pp. 799 – 802.
- [4] G. Fodor, C. Koutsimanis, A. Rác, N. Reider, A. Simonsson, and W. Müller, "Intercell interference coordination in OFDMA networks and in the 3GPP long term evolution system," *Journ. of Commun.*, pp. 445–453, Aug. 2009.
- [5] X. Mao, A. Maaref, and K. Teo, "Adaptive soft frequency reuse for inter-cell interference coordination in SC-FDMA based 3GPP LTE uplinks," in *Proc. IEEE Global Telecommun. Conf.*, Dec. 2008, pp. 36–46.
- [6] 3GPP TS 36.423 V8.8.0, "Evolved universal terrestrial radio access network (E-UTRAN): X2 application protocol (X2AP)," Dec. 2009.
- [7] R1-060877 Motorola, "Frequency domain scheduling for E-UTRA," 3GPP TSG RAN1#44, Athens, Mar. 2006.
- [8] F. Calabrese, C. Rosa, M. Anas, P. Michaelsen, K. Pedersen, and P. Mogensen, "Adaptive transmission bandwidth based packet scheduling for LTE uplink," in *Proc. IEEE Veh. Technol. Conf.*, Sep. 2008.
- [9] H. Myung, J. Lim, and D. Goodman, "Single carrier FDMA for uplink wireless transmission," *IEEE Veh. Technol. Mag.*, vol. 1, pp. 30 – 38, Sep. 2006.
- [10] 3GPP TS 36.214 V8.7.0, "Evolved universal terrestrial radio access (E-UTRA): Physical layer — measurements," Sep. 2009.
- [11] K. Brueninghaus, D. Astély, T. Sälzer, S. Visuri, A. Alexiou, S. Karger, and G.-A. Seraji, "Link performance models for system level simulations of broadband radio access systems," in *Proc. IEEE Int. Symp. Pers., Indoor and Mob. Radio Commun.*, Sep. 2005.
- [12] A. Müller and P. Frank, "Cooperative interference prediction for enhanced link adaptation in the 3GPP LTE uplink," in *Proc. IEEE Veh. Technol. Conf.*, May 2010.
- [13] 3GPP TR 25.814 V7.1.0, "Physical layer aspects for evolved universal terrestrial radio access (UTRA)," Sep. 2006.
- [14] 3GPP TS 36.211 V8.6.0, "Evolved universal terrestrial radio access (E-UTRA): Physical channels and modulation," Mar. 2009.